Original Research Article

On the existence of time delay for rotating beam with proportional–derivative controller

Abstract

A rotating beam at varying speed mathematical model is studied. Multiple time scales method is applied to the nonlinear system of differential equationsandinvestigated the system behavior approximate solution in the instance of resonance case.We studied the system in case of applying the delayed control on the displacement and the velocity with Proportional–derivative (PD) controller.The consistency of the steady state solution in the near-resonance case is reviewed and analyzed using the Routh-Huriwitz approach. The factors on the steady state solution of the various parameters are recognized and discussed. Simulation effects are obtained using MATLAB software package.Differentresponse curves are involved to showand compare controllereffects at various system parameters.

KeywordsNon-linear dynamical system, multiple time scales method, active feedback controller, time delay.

List of symbols

$X_1, \dot{X}_1, \ddot{X}_1$	Position, velocity and Acceleration of the system first mode.
$X_1, \dot{X}_1, \ddot{X}_1$	Position, velocity and Acceleration of the system second mode.
$\mu_i\ , i=1,2$	Damping parameters of the system modes
ω	System modes natural frequency
$\beta_{11}, \beta_{21}, \beta_{13}, \beta_{22}$	Coupling factors between the system modes
β_5	Cubic nonlinearity factor of the system modes
β_{14}, β_{24}	Parametric excitation parameters
f_o, f	Constant rotating speed and variable rotating speed
Ω	Excitation frequency
k_1, k_2	Controller feedback gains
σ_1, σ_2	Detuning parameters
τ	Time delay
ε	Small perturbation parameter
C_∞	denotes the speed of sound
ρ_∞	the density of the free stream air
X	the velocity of the free stream air

$\beta(z)=\beta_o z/L$	the pre-twist angle of a current beam cross section
β_o	the pre-twist at the beam tip
υ	the poisons ratio
E	Young's modulus
ΔT	the change in temperature from the reference level T_o.

1 Introduction

In dynamical and structural structures, disturbances and complex instability are always undesired phenomena. These systems face nonlinear vibrations for numerous purposes, such as materials' nonlinear properties, geometric nonlinearities, and nonlinear powers of excitation.Much time, money and efforts are spent on minimizing these systems' vibrations and oscillations for longer life and preventing them from failure or damage.

Many scholars and scientists have paid attention to and attempted to alleviate this topic that affects equipment, industry, and frugality. The high amplitude nonlinear vibration activity of a revolving cantilever beam is treated by Thomas et al.[1], with applications for turbo machinery and turbo-propeller blades.The effect of rotation speed on the nonlinear vibrations of the beam and particularly on the hardening/softening behavior of its resonances and the occurrence of high amplitude jump phenomena were investigated. A new dynamic model of a rotating flexible beam with a condensed mass positioned in an arbitrary location, based on the absolute nodal coordinate formulation, was investigated by Zhang et al.[2].They found that both the magnitude and the direction of the condensed mass impact the normal frequencies and the mode shapes. Aeroelastic analysis of a spinning wind turbine blade was conducted by Rezaei et al.[3] by considering the effects of geometrical nonlinearities associated with large blade deflection created during the operation of the wind turbine.Through applying the concepts of quasi-steady and unsteady airfoil aerodynamics, they proposed an aerodynamic model based on the strip theory. The results showed that geometrical nonlinearity, especially for larger structural deformations, had a significant impact.The effect of rotation velocity on nonlinear resonances is considered in[4], and the multi-scale perturbation approach is used and solved in the von Kármán[5] model. In order to simulate nonlinear resonances via a one-mode Galerkin expansion, nonlinear beam models such as axial inertia and nonlinear curvature are used.Nonlinear resonance curves are also computed, based on a Galerkin discretization with Legendre polynomials and a continuity process, with a completely numerical approach (harmonic balance coupled to an asymptotic numerical technique).For more detailed and effective dynamic analysis of a rotating cantilever beam with elastic deformation defined by partial integro-differential equations with non-Cartesian deformation variables, Kim and Chung[6] suggested a nonlinear model.They showed that the proposed model not only provided good numerical precision and efficiency, but also overcome the constraints expressed by Cartesian variables of a previous traditional nonlinear model. The dynamics of a structure consisting of a rotating rigid hub and a thin-walled composite beam with an embedded active part were introduced by Latalski [7].

Based on the device rotation velocity and laminae fiber orientation angle, they studied natural mode shapes and electrical field spatial distribution. A Proportional Derivative (PD) controller was applied by Kandil, H. El-Gohary[8] to research the effects of time delay on its output to decrease the oscillations of a spinning beam at different speeds.Although the vibrational modes of the dual system are linearly coupled, the controller is applied to only one mode and the other coupled mode tracks it. In the case of the worst resonance cases that were verified numerically, they regulated the device. Yao et al.[9, 10] applied the theory and isotropic constitutive law of Hamilton in order to infer the beam's governing equations.Of supersonic gas flow and high temperature, they studied the dynamics at different speeds. Choi et al.[11, 12] showed that an active damping effect can be obtained with polyvinylidene fluoride (PVDF) sensors and macrofiber composite (MFC) actuators through a negative velocity feedback control algorithm. MFC is a composite form of piezoelectric material.Through the required arrangement and distribution scale of the sensor/actuator pair, ample vibration suppression efficiency would therefore be obtained.

Joy Mondal, and S. Chatterjee [13]proposed the efficacy of velocity feedback based nonlinear resonant controller to control the free and forced self-excited vibration of a nonlinear beam. The control force is determined using the nonlinear function of the derivative of the filter vector, which is fed through a second-order filter with the velocity signal from the sensor. Liang Li et al. [14] has developed a new hierarchical model for vibration studies of rotating versatile beams with improved active constrained layer damping (EACLD) treatment that is partially shielded. The mass effect of the two added edge components is included by modeling the EACLD patch's edge element as an analogous spring with attached point mass. The assumed mode approach and Lagrange's equations are used to obtain the discrete rigid-flexible coupled dynamic equations of hub-beam systems with EACLD treatment in the open-loop and closed-loop situations.

Boumediène, and Smaoui [15] believed that the beam is to be non-uniform and clamped at its left end to the disk's core, where torque control occurs, while a memory boundary control resides at the right end. The standard torque control is first proposed, followed by the boundary control, which is designed using a special type of memory phenomenon as well as the input's dynamic features.L.F. Lyu, W.D. Zhu [16] demonstrated a new operational modal analysis (OMA) method for a rotating structure based on a rigorous rotating beam vibration theory, an image processing method, and the lifting method of data processing. They developed a novel tracking continuously scanning laser Doppler vibrometer (TCSLDV) method to monitor and scan a rotating structure, and image processing was used to determine the rotating structure's real-time location, enabling the TCSLDV system to track a time-varying scan direction on the rotating structure.

In this article, the PID control with time delay control are applied to the system of rotating beam at varying speeds shown in Figure 1a [8,9,10]subjected external and parametric forcein order to reduce its oscillations and enhance its efficiency. The displacements of the blade cross section are measured by using MFC sensors that are distributed over the bottom surface of the blade, as shown in Fig. 1b. The measured signals will be sent back to the computer to analyze and compute the appropriate control signal as shown in Fig. 1c. Once the control signal is calculated, it is passed through conditioning circuit and then be applied to the embedded MFC actuators that are distributed over the top of the blade so that they can modify the blade position and reduce its vibration, a control loop feedback mechanism illustrated in figure 2 are continuously calculates an error value e(t) as the difference between a desired setpoint (SP) and a measured process variable (PV) and applies a correction based on proportional, integral, and derivative terms (denoted P, I, and D respectively).The multiple time scales perturbation technique (MSPT) was applied to obtain an approximate solution and showing the response equation. The stability of the system at primary and principle parametric resonance case is investigated using both of phase plane and frequency response equation. The numerical solution and the effect of the different parameters for the response of the nonlinear dynamic system.

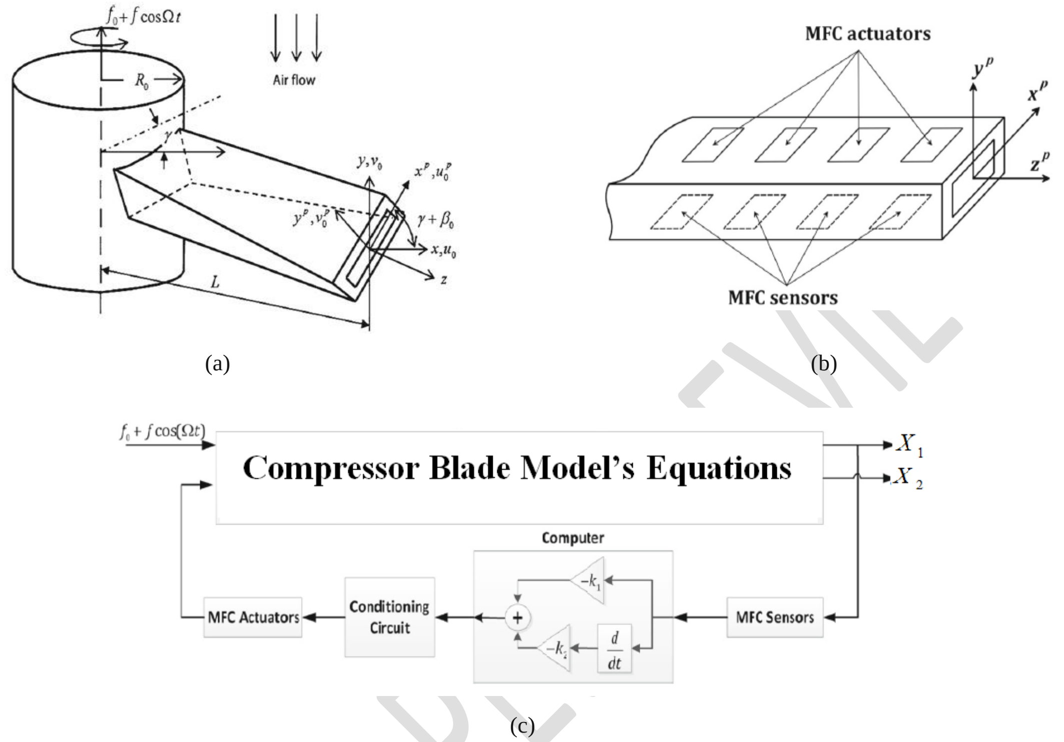

Figure 1 Rotating compressor blade model, (a) thin-walled pre-twisted blade, (b) sensors and actuators distribution and (c) block diagram of control process.

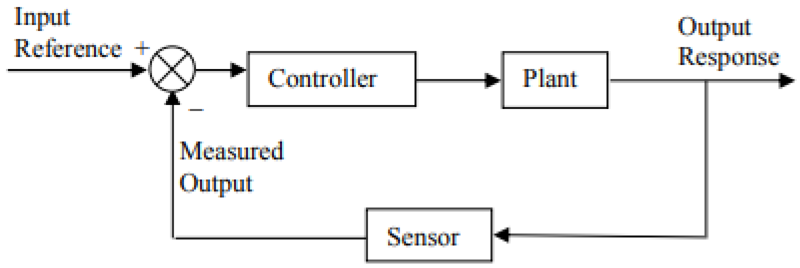

Figure 2 A closed loop system controller.

2 System model and mathematical analysis

The equations of motion for the rotating beam shown in figure 1 is introduced by Bekhoucha [5] and Yao et al. [9, 10] by applying the Hamilton's principle as:

$$\int_0^t (\delta K - \delta U + \delta W)\, dt\ , \qquad (1)$$

where$K$ denote the kinetic energy, U the strain energy, and W is the virtual work of external forces, t denotes time, and δ is the variation operator. By calculating the variation in kinetic, strain energy, and the virtual work of non-conservative external forces (given in Appendix),and substituting Equation (1), then the governing equations of the nonlinear vibration system for the rotating beam are as the following:

$$
\begin{aligned}
&\ddot{u}-\Omega^2\left[u+R(z)u''+R'(z)u'\right]+\alpha\,\Delta T\,u''-\left[a_1(z)v''-a_3(z)u''\right]''\\
&=u'\left[u'u''+v'v''\right]+u''\left[\frac{1}{2}(u')^2+\frac{1}{2}(v')^2\right]-\dot{\Omega}(R_o+z)+p_x,\\
&\ddot{v}-\Omega^2\left[R(z)v''+R'(z)v'\right]+\alpha\,\Delta T\,v''-\left[a_1(z)u''-a_2(z)v''\right]''\\
&=v'\left[u'u''+v'v''\right]+v''\left[\frac{1}{2}(u')^2+\frac{1}{2}(v')^2\right]+p_y,
\end{aligned}
\qquad (2)
$$

where$u$, v are the translations along the x, and y axes, p_x, p_y are the external forces per unit axial length in the x and the y direction. The values of p_x, p_y and the variables $a_i(z), i=1,2,3,$ are given in Appendix. The dots and primes, respectively, represent partial differentiation with respect to t and z, $R(X,Y,Z)$ is the vector function of a point $M(X,Y,Z)$ of the deformed thin wall beam, and given by $R(X,Y,Z)=(X+u)i+(Y+v)j+Z\,k+R_o$. Applying Galerkin's approach [20] on system (2), the horizontal and vertical displacements u,v have been approximated to the modes X_1, X_2 respectively to have the dimensionless two degree of freedom non-linear rotating beam system in the form:

$$
\begin{aligned}
&\ddot{X}_1+2\mu_1\dot{X}_1+\omega^2X_1+\beta_{13}\dot{X}_2+\beta_{11}X_2+\beta_5X_1X_2^2+\beta_5X_1^3=2f_of\,\beta_{14}X_1\cos(\Omega t)\\
&+f^2\beta_{14}X_1\cos^2(\Omega t)+f\,\beta_{16}\Omega\sin(\Omega t)-k_1X_1(t-\tau)-k_2\dot{X}_1(t-\tau),
\end{aligned}
\qquad (3a)
$$

$$
\begin{aligned}
&\ddot{X}_2+2\mu_2\dot{X}_2+\omega^2X_2+\beta_{22}\dot{X}_1+\beta_{21}X_1+\beta_5X_2X_1^2+\beta_5X_2^3=2f_of\,\beta_{24}X_2\cos(\Omega t)\\
&+f^2\beta_{24}X_2\cos^2(\Omega t),
\end{aligned}
\qquad (3b)
$$

where all system parameters are defined before.

Scaling the previous parameters as:

$$
\begin{aligned}
&\beta_{11}=\varepsilon\hat{\beta}_{11},\beta_{13}=\varepsilon\hat{\beta}_{13},\beta_{14}=\varepsilon\hat{\beta}_{14},\beta_{16}=\varepsilon\hat{\beta}_{16},\beta_{21}=\varepsilon\hat{\beta}_{21},\beta_{22}=\varepsilon\hat{\beta}_{22},\beta_{24}=\varepsilon\hat{\beta}_{24},\beta_5=\varepsilon\hat{\beta}_5,\\
&k_1=\varepsilon\hat{k}_1,k_2=\varepsilon\hat{k}_2,\mu_1=\varepsilon\hat{\mu}_1,\mu_2=\varepsilon\hat{\mu}_2.
\end{aligned}
\qquad (4)
$$

Applying multiple time scales method [17], an asymptotic expansion is sought as:

$$
\begin{aligned}
&X_1(T_o,T_1,\varepsilon)=X_{10}(T_o,T_1)+\varepsilon X_{11}(T_o,T_1)+O(\varepsilon^2),\\
&X_2(T_o,T_1,\varepsilon)=X_{20}(T_o,T_1)+\varepsilon X_{21}(T_o,T_1)+O(\varepsilon^2),\\
&X_1(T_o-\tau,T_1-\varepsilon\tau,\varepsilon)=X_{10\tau}(T_o,T_1)+\varepsilon X_{11\tau}(T_o,T_1)+O(\varepsilon^2),
\end{aligned}
\qquad (5)
$$

where the time derivative will takes the values:

$$\frac{d}{dt}=D_0+\varepsilon D_1+O(\varepsilon^2),\frac{d^2}{dt^2}=D_o^2+2\varepsilon D_0 D_1+O(\varepsilon^2) \quad (6)$$

and $T_n=\varepsilon^n t,\ D_n=\frac{\partial}{\partial T_n}, n=0,1$.

Applying Eqs. (4)-(6) into Eq. (3),then equating same powers of ε coefficients to obtain the following:

$$O(\varepsilon^0):(D_o^2+\omega^2)X_{10}=0 \quad (7a)$$

$$(D_o^2+\omega^2)X_{20}=0 \quad (7b)$$

$O(\varepsilon)$:

$$\begin{aligned}(D_o^2+\omega^2)X_{11}&=\hat{\beta}_{14}f\ X_{10}\cos(\Omega T_0)[2f_o+f\ \cos(\Omega T_0)]+f\ \hat{\beta}_{16}\Omega\sin(\Omega T_0)\\&-2D_0D_1X_{10}-2\hat{\mu}_1D_0X_{10}-\hat{\beta}_{13}D_0X_{20}-\hat{\beta}_{11}X_{20}-\hat{\beta}_5X_{10}X_{20}^2-\hat{\beta}_5X_{10}^3\\&-k_1X_{10}-k_2D_0X_{10}-\hat{k}_1X_{10\tau}-\hat{k}_2D_0X_{10\tau}.\end{aligned} \quad (8a)$$

$$\begin{aligned}(D_o^2+\omega^2)X_{21}&=\hat{\beta}_{24}f\ X_{20}\cos(\Omega T_0)[2f_o+f\ \cos(\Omega T_0)]-2D_0D_1X_{20}-2\hat{\mu}_2D_0X_{20}\\&-\hat{\beta}_{22}D_0X_{10}-\hat{\beta}_{21}X_{10}-\hat{\beta}_5X_{20}X_{10}^2-\hat{\beta}_5X_{20}^3.\end{aligned} \quad (8b)$$

It is well known that solutions of (7a), (7b) are

$$\begin{aligned}X_{10}&=A(T_1)e^{i\omega T_0}+cc.,\\X_{20}&=B(T_1)e^{i\omega T_0}+cc.,\\X_{10\tau}&=A_\tau(T_1)e^{i\omega(T_0-\tau)}+cc.,\end{aligned} \quad (9)$$

Using Taylor expansion, then the value of $A_\tau(T_1)$ is given by[21]:

$$A_\tau(T_1)=A(T_1-\varepsilon\tau)=A(T_1)-\varepsilon\tau\dot{A}(T_1)+\cdots$$

As approximation, we keep only the first term of this expansion, then, $X_{10\tau}=A(T_1)e^{i\omega(T_0-\tau)}+cc.$,

where $cc.$ represents the complex conjugates of the preceding terms and A,B are complex functions of T_1.

Now we will study the system worst operating modes due to resonance cases.

Case 1 Primary resonance:

The primary resonance occur when the value of Ω is equal to ω so we study the behavior of the system near this case i.e.

$$\Omega=\omega+\sigma_1=\omega+\varepsilon\hat{\sigma}_1, \quad (10)$$

Combining Eq.(9) and (10) into (8), we get:

$$
\begin{aligned}
(D_o^2+\omega^2)X_{11} &= -2D_o D_1(A e^{i\omega T_o}+\bar{A}e^{-i\omega T_o})-2\mu_1 D_o(B e^{i\omega T_o}+\bar{B}e^{-i\omega T_o})\\
&-\beta_{13}D_o(B e^{i\omega T_o}+\bar{B}e^{-i\omega T_o})-\beta_{11}(B e^{i\omega T_o}+\bar{B}e^{-i\omega T_o})\\
&-\beta_5(A e^{i\omega T_o}+\bar{A}e^{-i\omega T_o})(B e^{i\omega T_o}+\bar{B}e^{-i\omega T_o})^2-\beta_5(A e^{i\omega T_o}+\bar{A}e^{-i\omega T_o})^3\\
&+f_o f\,\beta_{14}(A e^{i\omega T_o}+\bar{A}e^{-i\omega T_o})(e^{i(\omega+\sigma_1)T_o}+e^{-i(\omega+\sigma_1)T_o})\\
&+\frac{f^2\beta_{14}}{4}(A e^{i\omega T_o}+\bar{A}e^{-i\omega T_o})(e^{i(\omega+\sigma_1)T_o}+e^{-i(\omega+\sigma_1)T_o})^2\\
&-\frac{i f\,\beta_{16}(\omega+\sigma_1)}{2}(e^{i(\omega+\sigma_1)T_o}-e^{-i(\omega+\sigma_1)T_o})-k_1(A e^{i\omega(T_o-\tau)}+\bar{A}e^{-i\omega(T_o-\tau)})\\
&-k_2 D_o(A e^{i\omega(T_o-\tau)}+\bar{A}e^{-i\omega(T_o-\tau)}),
\end{aligned}
\tag{11}
$$

$$
\begin{aligned}
(D_o^2+\omega^2)X_{21} &= -2D_o D_1(B e^{i\omega T_o}+\bar{B}e^{-i\omega T_o})-2\mu_2 D_o(B e^{i\omega T_o}+\bar{B}e^{-i\omega T_o})\\
&-\beta_{22}D_o(A e^{i\omega T_o}+\bar{A}e^{-i\omega T_o})-\beta_{21}(A e^{i\omega T_o}+\bar{A}e^{-i\omega T_o})\\
&-\beta_5(B e^{i\omega T_o}+\bar{B}e^{-i\omega T_o})(A e^{i\omega T_o}+\bar{A}e^{-i\omega T_o})^2-\beta_5(B e^{i\omega T_o}+\bar{B}e^{-i\omega T_o})^3\\
&+f_o f\,\beta_{24}(B e^{i\omega T_o}+\bar{B}e^{-i\omega T_o})(e^{i(\omega+\sigma_1)T_o}+e^{-i(\omega+\sigma_1)T_o})\\
&+\frac{f^2\beta_{24}}{4}(B e^{i\omega T_o}+\bar{B}e^{-i\omega T_o})(e^{i(\omega+\sigma_1)T_o}+e^{-i(\omega+\sigma_1)T_o})^2\\
&-\frac{i f\,\beta_{16}(\omega+\sigma_1)}{2}(e^{i(\omega+\sigma_1)T_o}-e^{-i(\omega+\sigma_1)T_o})-k_1(A e^{i\omega(T_o-\tau)}+\bar{A}e^{-i\omega(T_o-\tau)})\\
&-k_2 D_o(A e^{i\omega(T_o-\tau)}+\bar{A}e^{-i\omega(T_o-\tau)}).
\end{aligned}
\tag{12}
$$

Eliminating all secular terms in Eqs. (11), and (12), we obtain:

$$
\begin{aligned}
&\frac{\beta_{14}f^2}{2}(A+\bar{A}\frac{e^{2i\sigma_1 t}}{2})-2i\,\omega\dot{A}-2i\,\mu_1\omega A-\beta_{11}B-i\,\omega\beta_{13}B-2\beta_5 AB\bar{B}-3\beta_5 A^2\bar{A}\\
&-\beta_5 B^2\bar{A}-0.5i\,\beta_{16}\Omega f e^{i\sigma_1 t}-k_1 A e^{-i\omega\tau}-i\,k_2\omega A e^{-i\omega\tau}=0,
\end{aligned}
\tag{13}
$$

$$
\frac{\beta_{24}f^2}{2}(B+\bar{B}\frac{e^{2i\sigma_1 t}}{2})-2i\,\omega\dot{B}-2i\,\mu_2\,\omega B-\beta_{21}A-i\,\omega\beta_{22}A-2\beta_5 AB\bar{A}-3\beta_5 B^2\bar{B}-\beta_5 A^2\bar{B}=0
\tag{14}
$$

Converting A,B to the polar form then we have:

$$
A=\frac{a_1}{2}e^{i\beta_1},\qquad B=\frac{a_2}{2}e^{i\beta_2}
\tag{15}
$$

where $a_j,\beta_j,(j=1,2)$ are the system amplitude and phase respectively.

Introducing Eq. (15) in Eqn. (13) and (14)and equating the real and imaginary parts we get:

$$
\begin{aligned}
\dot{a}_1 &= -\mu_1 a_1-\frac{\beta_{11}a_2}{2\omega}\sin(\varphi_2)-\frac{\beta_{13}a_2}{2}\cos(\varphi_2)+\frac{\beta_5 a_1 a_2^2}{8\omega}\sin(2\varphi_2)\\
&+\frac{\beta_{14}a_1 f^2}{8\omega}\sin(2\varphi_1)-\frac{\beta_{16}f\,\Omega}{2\omega}\cos(\varphi_1)+\frac{k_1 a_1}{2\omega}\sin(\omega\tau)-\frac{k_2 a_1}{2}\cos(\omega\tau),
\end{aligned}
\tag{16a}
$$

$$\dot{\varphi}_1 = \sigma_1 - \frac{\beta_{11} a_2}{2\omega a_1}\cos(\varphi_2) + \frac{\beta_{13} a_2}{2a_1}\sin(\varphi_2) - \frac{\beta_5 a_2^2}{8\omega}\cos(2\varphi_2) - \frac{\beta_5 a_2^2}{4\omega}$$
$$-\frac{3\beta_5 a_1^2}{8\omega} + \frac{\beta_{14} f^{\,2}}{4\omega}(1 + \frac{\cos(2\varphi_1)}{2}) + \frac{\beta_{16}\Omega f}{2\omega a_1}\sin(\varphi_1) - \frac{k_1}{2\omega}\cos(\omega\tau) - \frac{k_2}{2}\sin(\omega\tau)\,, \quad (16b)$$

$$\dot{a}_2 = -\mu_2 a_2 + \frac{\beta_{21} a_1}{2\omega}\sin(\varphi_2) - \frac{\beta_{22} a_1}{2}\cos(\varphi_2) + \frac{\beta_5 a_2 a_1^2}{8\omega}\sin(2\varphi_2)$$
$$-\frac{\beta_{24} a_2 f^{\,2}}{8\omega}\sin(2\varphi_2 - 2\varphi_1)\,, \quad (16c)$$

$$\dot{\varphi}_2 = \sigma_1 + \frac{\beta_{22} a_1}{2a_2}\sin(\varphi_2) - \frac{\beta_{21} a_1}{2\omega a_2}\cos(\varphi_2) + \frac{\beta_5}{4\omega}(a_1^2 - a_2^2) + \frac{\beta_5}{8\omega}(a_1^2 - a_2^2)\cos(2\varphi_2)$$
$$-\frac{3\beta_5}{8\omega}(a_1^2 - a_2^2) - \frac{\beta_{24} f^{\,2}}{8\omega}\cos(2\varphi_2 - 2\varphi_1) + \frac{f^{\,2}}{4\omega}(\beta_{14} - \beta_{24}) + \frac{\beta_{13} a_2}{2a_1}\sin(\varphi_2) \quad (16d)$$
$$-\frac{\beta_{11} a_2}{2\omega a_1}\cos(\varphi_2) + \frac{\beta_{14} f^{\,2}}{8\omega}\cos(2\varphi_1) + \frac{\beta_{16}\Omega f}{2\omega a_1}\sin(\varphi_1) - \frac{k_1}{2\omega}\,.$$

where

$$\varphi_1 = \sigma_1 t - \beta_1\,, \qquad \varphi_2 = \beta_2 - \beta_1\,. \quad (17)$$

For obtaining the steady state solution for amplitude and phase, putting $\dot{a}_1 = \dot{\varphi}_1 = \dot{a}_2 = \dot{\varphi}_2 = 0$ into Eq.(16),the resultant formulas can be solved numerically. To discuss the stability behavior of these solutions, linearizing these equations according to Lyapunov first (indirect) method [18] to give the following system:

$$\begin{bmatrix} \dot{a}_1 \\ \dot{\varphi}_1 \\ \dot{a}_2 \\ \dot{\varphi}_2 \end{bmatrix} = \begin{bmatrix} \frac{\partial \dot{a}_1}{\partial a_1} & \frac{\partial \dot{a}_1}{\partial \varphi_1} & \frac{\partial \dot{a}_1}{\partial a_2} & \frac{\partial \dot{a}_1}{\partial \varphi_2} \\ \frac{\partial \dot{\varphi}_1}{\partial a_1} & \frac{\partial \dot{\varphi}_1}{\partial \varphi_1} & \frac{\partial \dot{\varphi}_1}{\partial a_2} & \frac{\partial \dot{\varphi}_1}{\partial \varphi_2} \\ \frac{\partial \dot{a}_2}{\partial a_1} & \frac{\partial \dot{a}_2}{\partial \varphi_1} & \frac{\partial \dot{a}_2}{\partial a_2} & \frac{\partial \dot{a}_2}{\partial \varphi_2} \\ \frac{\partial \dot{\varphi}_2}{\partial a_1} & \frac{\partial \dot{\varphi}_2}{\partial \varphi_1} & \frac{\partial \dot{\varphi}_2}{\partial a_2} & \frac{\partial \dot{\varphi}_2}{\partial \varphi_2} \end{bmatrix} \begin{bmatrix} a_1 \\ \varphi_1 \\ a_2 \\ \varphi_2 \end{bmatrix}$$
$$= \begin{bmatrix} \gamma_{11} & \gamma_{12} & \gamma_{13} & \gamma_{14} \\ \gamma_{21} & \gamma_{22} & \gamma_{23} & \gamma_{24} \\ \gamma_{31} & \gamma_{32} & \gamma_{33} & \gamma_{34} \\ \gamma_{41} & \gamma_{42} & \gamma_{43} & \gamma_{44} \end{bmatrix} \begin{bmatrix} a_1 \\ \varphi_1 \\ a_2 \\ \varphi_2 \end{bmatrix} = [J] \begin{bmatrix} a_1 \\ \varphi_1 \\ a_2 \\ \varphi_2 \end{bmatrix} \quad (18)$$

where the values of $\gamma_{mn}, (m, n = 1, 2, 3, 4)$ are included in "Appendix". Stability of a particular fixed point with respect to perturbation proportional to $\exp(\lambda T_1)$ is determined by zeros of characteristic equation of the jacobian determinate $|J - \lambda I|$ which gives:

$$\lambda^4 + \Pi_1 \lambda^3 + \Pi_2 \lambda^2 + \Pi_3 \lambda + \Pi_4 = 0, \quad (19)$$

where $\Pi_{mn}, m, n = 1:4$ are given in appendix.According to Routh-Hurwitze criteria [18, 19], the necessary and sufficient condition for all characteristic roots of the characteristic equation (19) to have negative real parts if and only if the determinate D and all its principle minors are positive, where $D = \begin{vmatrix} \Pi_1 & 1 & 0 & 0 \\ \Pi_3 & \Pi_2 & \Pi_1 & 1 \\ 0 & \Pi_4 & \Pi_3 & \Pi_2 \\ 0 & 0 & 0 & \Pi_4 \end{vmatrix}$, then the stability conditions will be

$$\Pi_1 > 0,\ \Pi_4 > 0,\ (\Pi_1\Pi_2 - \Pi_3) > 0,\ [\Pi_3(\Pi_1\Pi_2 - \Pi_3) - \Pi_1^2\,\Pi_4] > 0, \quad (20)$$

Case 2 Principal parametric resonance

Assume that the detuning parameter σ_2 is to be used to depict the principal parametric resonance as shown in the following relation:

$$\Omega = 2\omega + \sigma_2 = 2\omega + \varepsilon\hat{\sigma}_2 \quad (21)$$

Similarly as in case 1 combining Eq. (9) and (21) into (8) andeliminating all secular terms from the resulting equations to have:

$$\frac{\beta_{14} f^{2}}{2} A + \beta_{14} f_o f\, \bar{A}\frac{e^{i\sigma_2 t}}{2} - 2i\,\omega\dot{A} - 2i\,\mu_1\,\omega A - \beta_{11}B - i\,\omega\beta_{13}B$$
$$-2\beta_5\, A\, B\, \bar{B} - 3\beta_5\, A^2\bar{A} - \beta_5\, B^2\bar{A} - k_1 A\, e^{-i\,\omega\tau} - i\, k_2\,\omega A\, e^{-i\,\omega\tau} = 0, \quad (22a)$$

$$\beta_{24} f\,(\frac{B\, f}{2} + f_o\,\bar{B}\, e^{i\sigma_2 t}) - 2i\,\omega\dot{B} - 2i\,\mu_2\,\omega B - \beta_{21}A - i\,\omega\beta_{22}A$$
$$-2\beta_5 A\, B\, \bar{A} - 3\beta_5 B^2\bar{B} - \beta_5 A^2\bar{B} = 0 \quad (22b)$$

Using Eq. (15) into (22) and equating the real and imaginary parts to obtain the following system of ordinary differential equations:

$$\dot{a}_1 = -\mu_1 a_1 - \frac{\beta_{11}\, a_2}{2\omega}\sin(\varphi_2) - \frac{\beta_{13}\, a_2}{2}\cos(\varphi_2)$$
$$-\frac{\beta_5\, a_1 a_2^2}{4\omega}\sin(2\varphi_2) + \frac{\beta_{14}\, f_o\, f}{2\omega}\sin(\varphi_1) - \frac{k_1\, a_1}{2\,\omega}\sin(\omega\tau) - \frac{k_2\, a_1}{2}\cos(\omega\tau) \quad (23a)$$

$$\dot{\varphi}_1 = \sigma_2 - \frac{\beta_{11}\, a_2}{\omega\, a_1}\cos(\varphi_2) + \frac{\beta_{13}\, a_2}{a_1}\sin(\varphi_2) - \frac{\beta_5\, a_2^2}{2\,\omega}\cos(2\varphi_2)$$
$$-\frac{\beta_5\, a_2^2}{2\,\omega} - \frac{3\beta_5\, a_1^2}{4\,\omega} + \frac{\beta_{14}\, f}{\omega}(\frac{f}{2} + f_o\cos(\varphi_1)) - \frac{k_1}{\omega}\cos(\omega\tau) - k_2\sin(\omega\tau), \quad (23b)$$

$$\dot{a}_2 = -\mu_2\, a_2 + \frac{\beta_{21}\, a_1}{2\omega}\sin(\varphi_2) - \frac{\beta_{22}\, a_1}{2}\cos(\varphi_2) + \frac{\beta_5\, a_2 a_1^2}{8\omega}\sin(2\varphi_2)$$
$$+\frac{\beta_{24}\, a_2 f_o\, f}{2\,\omega}\sin(\varphi_1 - 2\varphi_2), \quad (23c)$$

$$\dot{\varphi}_2 = \frac{\beta_{22}\, a_1}{2a_2}\sin(\varphi_2) + \frac{\beta_{21}\, a_1}{2\,\omega\, a_2}\cos(\varphi_2) + \frac{\beta_5\, a_1^2}{4\omega}(1 + \frac{\cos(2\varphi_2)}{2}) + \frac{3\beta_5\, a_2^2}{8\,\omega}$$
$$- \frac{\beta_{24} f_o\, f}{2\omega}\cos(\varphi_1 - 2\varphi_2) + \frac{f^{\,2}}{4\omega}\beta_{24} - \frac{\beta_{11}\, a_2}{2\,\omega\, a_1}\cos(\varphi_2) + \frac{\beta_{13}\, a_2}{2\, a_1}\sin(\varphi_2)$$
$$- \frac{\beta_5\, a_2^2}{4\,\omega}\cos(2\varphi_2) - \frac{\beta_5\, a_2^2}{4\,\omega} - \frac{3\beta_5\, a_1^2}{8\,\omega} + \frac{\beta_{14}\, f}{2\,\omega}(\frac{f}{2} + f_o\cos(\varphi_1)) - \frac{k_1}{2\,\omega}. \qquad (23d)$$

where

$$\varphi_1 = \sigma_2 t - 2\beta_1, \quad \varphi_2 = \beta_2 - \beta_1. \qquad (24)$$

Similarly For obtaining the steady state solution for amplitude and phase putting $\dot{a}_1 = \dot{\varphi}_1 = \dot{a}_2 = \dot{\varphi}_2 = 0$ into Eq. (23), the resultant formulas can be solved numerically using MATLAB software.

To discuss the stability behavior of these solutions, linearizing these equations according to Lyapunov first (indirect) method to give the following system:

$$\begin{bmatrix} \dot{a}_1 \\ \dot{\varphi}_1 \\ \dot{a}_2 \\ \dot{\varphi}_2 \end{bmatrix} = \begin{bmatrix} \zeta_{11} & \zeta_{12} & \zeta_{13} & \zeta_{14} \\ \zeta_{21} & \zeta_{22} & \zeta_{23} & \zeta_{24} \\ \zeta_{31} & \zeta_{32} & \zeta_{33} & \zeta_{34} \\ \zeta_{41} & \zeta_{42} & \zeta_{43} & \zeta_{44} \end{bmatrix} \begin{bmatrix} a_1 \\ \varphi_1 \\ a_2 \\ \varphi_2 \end{bmatrix} \qquad (25)$$

where the values of $\zeta_{mn}, (m, n = 1,2,3,4)$ are given in "Appendix". Numerically, primary resonance is the worst resonance case that is taken into account in the discussions.

3Results and discussion

In this section,system behaviors of the amplitude and phase at various resonance cases are illustrated. A comparison between active and time delay control and the effect of some system parameters on its amplitude are shown.

3.1 time history

Figure3(a, b) shows the time response for the amplitude X_1, X_2, where figure 3 (c) illustrates the system phase plane,Without resonance case and without applying any control system (i.e. $k_1 = k_2 = 0$)at the following parameter variables:

$$\omega = 65,\ \Omega = 100,\ \mu_1 = \mu_2 = 0.5,\ \beta_{11} = -0.003,\ \beta_{13} = -0.82,\ \beta_{14} = 0.55, \beta_{16} = 6.55,$$
$$\beta_5 = 0.9,\ \beta_{22} = -0.82,\ \beta_{21} = -0.001,\ \beta_{24} = 0.5,\ f_o = 7,\ f = 2,\ \tau = 0.$$

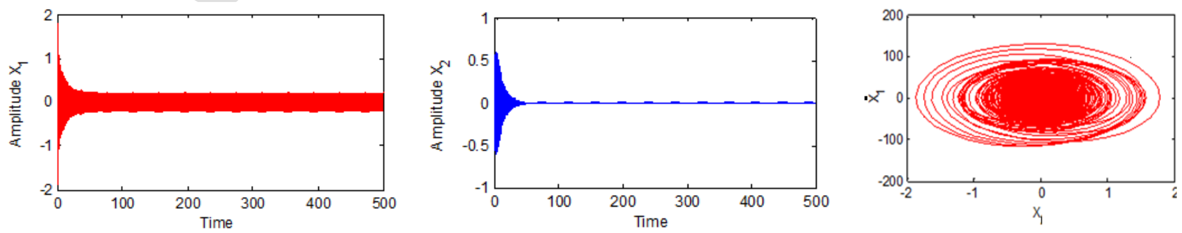

Fig. 3 (a) the time response for the amplitude X_1.

Fig. 3 (b) the time response for the amplitude X_2.

Fig. 3 (c)system phase plane

We can see that the steady state amplitudes are stable in the case of non-resonance operating mode. Figure 4clarifies the time history without control and with primary resonance at the same previous parameters except that $\Omega = \omega = 99$, we observe that the amplitudeshave been increased due to the resonance operating point.

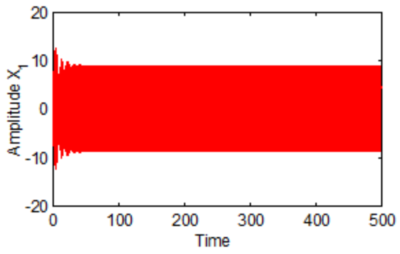

Fig. 4 (a) the time response for the Amplitude X_1.

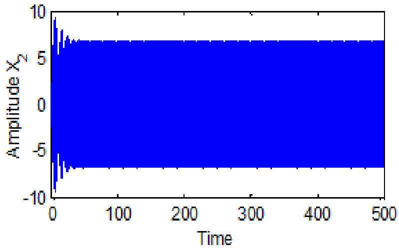

Fig. 4 (b) the time response for the amplitude X_2

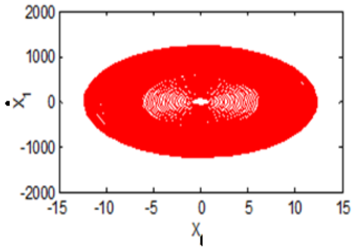

Fig. 4 (c)system phase plane

Now applying active and time delay control for the system with primary resonance and comparing the amplitudes.Figure 5, 6 shows the effect of active and time delay control on both X_1, X_2. We observe that the effective of active control is about 105%, and Time delay controller is about 125% so the time delay controller is more efficient than active velocity feed-back controller for this system.

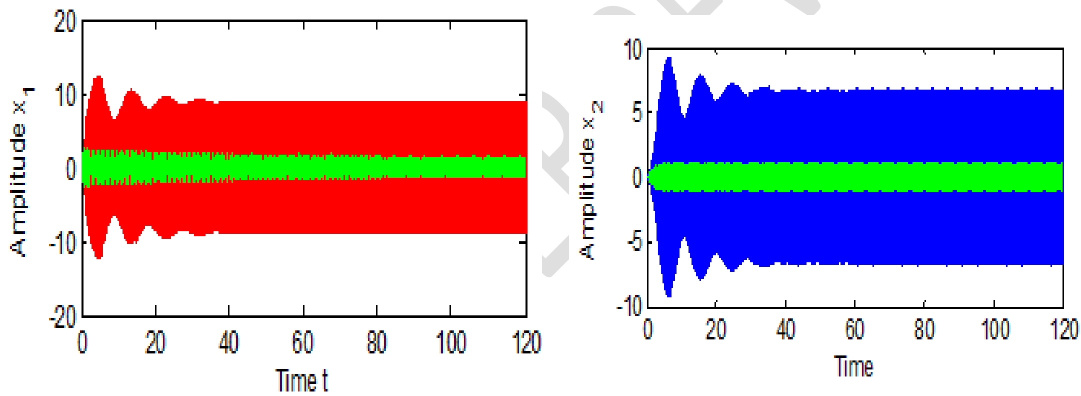

Figure 5 (a, b) effect of active control on x_1, x_2 respectively at primary resonance case.

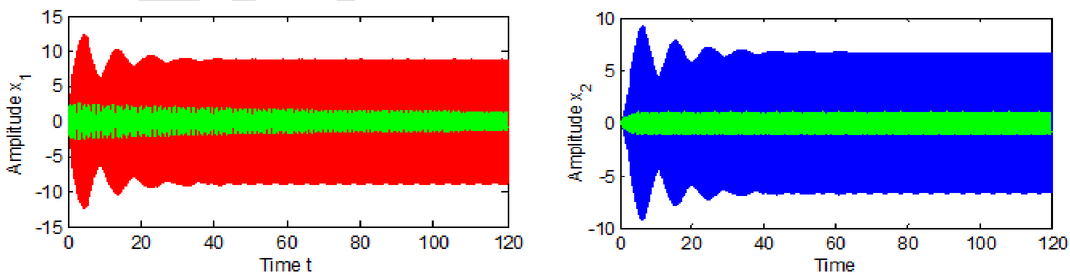

Figure 6 (a, b) effect of time delay controlon x_1, x_2 respectively at primary resonance case, $\tau = 0.0015$.

3.2comparisons with numerical method

In this sub-section we compared the approximate solution induced by (MTSM) and numerical solution using Rung-Kutta Method (RKM). Figure 7, and 8 show good agreement between the approximate solution (blue curves) and the numerical results (red curves) in case of $\tau = 0$, 0.0015 respectively.

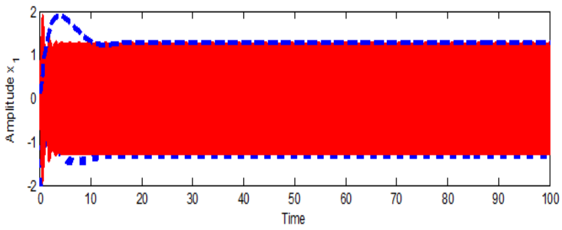

Fig. 7 (a) Time history for the amplitude X_1 using MTSM (blue curve) and RKM(red curve).

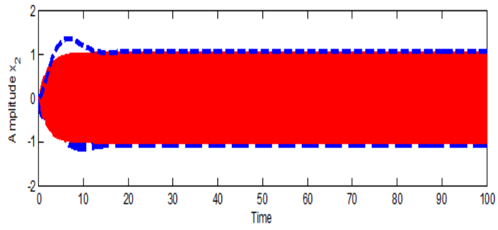

Fig. 7 (b) Time history for the amplitude X_2 using RKM (blue curve) and MTSM (red curve).

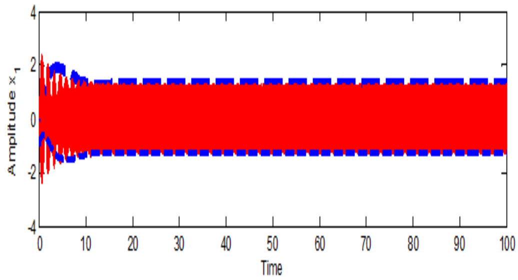

Fig. 8 (a) Time history for the amplitude X_1 using MTSM (blue curve) and RKM(red curve) for $\tau = 0.0015$.

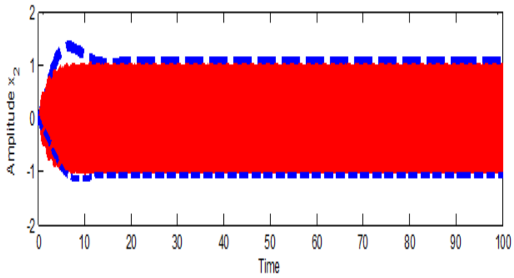

Fig. 8 (b) Time history for the amplitude X_2 using MTSM (blue curve) and RKM(red curve) for $\tau = 0.0015$.

3.3Frequency response

Now the following figures show the system amplitude against the detuning parameter σ_1 with change in specified values for system parameters. In figure 9 the parameters a_1, a_2 with σ_1 in case of primary resonance case with:

$$\omega = \Omega = 100,\ \mu_1 = 0.9, \mu_2 = 0.7,\ \beta_{11} = -0.003,\ \beta_{13} = -0.82,\ \beta_{14} = 0.55, \beta_{16} = 6.55,$$
$$\beta_5 = 0.9, \beta_{22} = -0.82,\ \beta_{21} = -0.001,\ \beta_{24} = 0.5,\ f_o = 7, f = 3,\ \tau = 0.0015, \varepsilon = 0.001,$$
$$k_1 = 1000, k_2 = 0.7, 1, 1.5.$$

We observe that the amplitude decreases with the increase of the gain k_2, then the delayed velocity feedback control is more efficient than the delay on the displacement. Figures10, and11 illustrate the effect of σ_1 on the amplitude with various values of the damping parameter μ_1, μ_2 as given in these figuresrespectively.The same system parameters values as given for figure9 are usedand $k_2 = 1$.We observe in fig. 10that the values of a_1, a_2 are proportional inversely with the damping parameter μ_1 but in fig. 11 the value of a_1 is approximatelyconstant with μ_2 as it is effect on the velocity $\dot{X}_2$ of the system second mode with two peaks.

3.4Amplitude vs. certain system parameters

Let us consider the parameters given in sub-section 3.3 unless otherwise specified.In this sub-section weshows the change of amplitude range with varying of the constant and variable rotating forces f_o, f as shown in figure 12 (a, b) respectively $\omega = 15, k_2 = 100$, $\Omega = 90$. The steady state amplitude of the main system is a monotonic increasing function of the excitation amplitude up to maximum amplitude at saturation. The saturation value may lead to an unstable or damaged system due to its large value. Figure 13 (a, b) describe the behavior of the amplitude with damping parameters μ_1, μ_2 respectivelyat $\Omega = \omega = 10$. We observe in figure 13 that the suitable range for $\mu_2 \leq 0.003$, and $\mu_1 \geq 0.2$, it is useful for the system to choose a large value for μ_1, but an expensive material should be used, so we use suitable materials with appropriate cost and adding a specified controller for reducing the amplitude for minimum values in the instance of resonance cases.

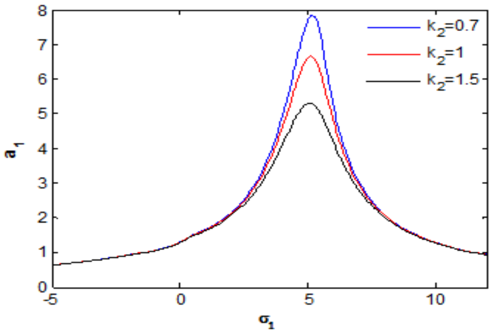

Fig. 9 (a) System amplitude a_1 against detuning parameter σ_1 at $k_2 = 0.7, 1, 1.5$.

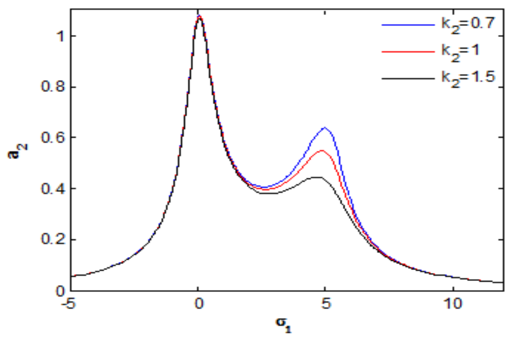

Fig. 9 (b) System amplitude a_2 against detuning parameter σ_1 at $k_2 = 0.7, 1, 1.5$.

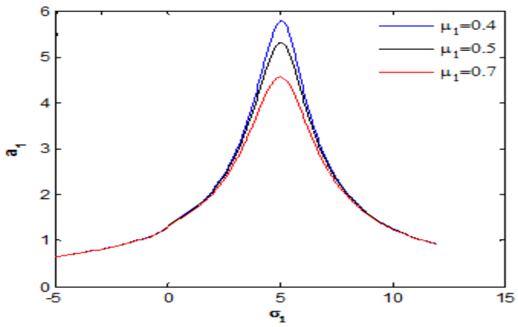

Fig. 10 (a) System amplitude a_1 against detuning parameter σ_1 at $\mu_1 = 0.4, 0.5, 0.7$.

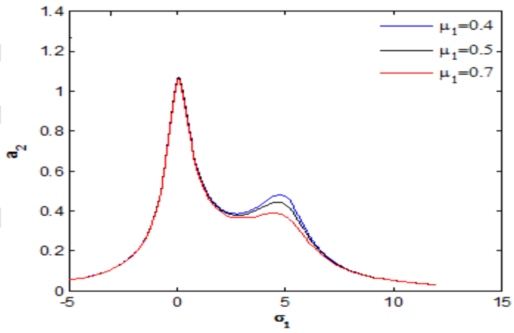

Fig. 10 (b) System amplitude a_2 against detuning parameter σ_1 at $\mu_1 = 0.4, 0.5, 0.7$.

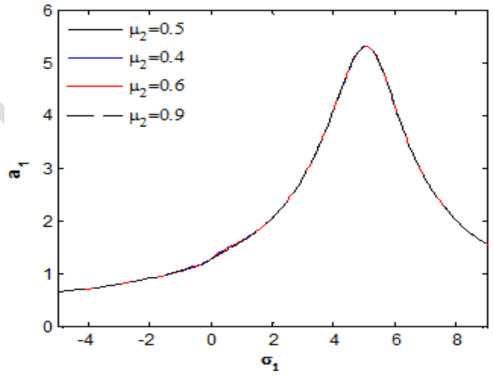

Fig. 11 (a) System amplitude a_1 against detuning parameter σ_1 at $\mu_2 = 0.4, 0.5, 0.6, 0.9$.

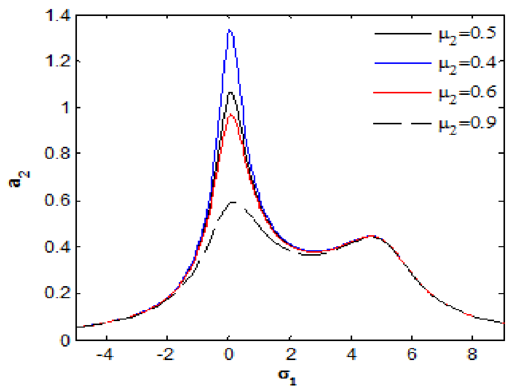

Fig. 11 (b) System amplitude a_2 against detuning parameter σ_1 at $\mu_2 = 0.4, 0.5, 0.6, 0.9$.

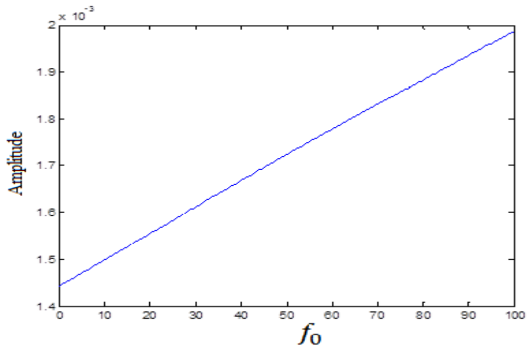

Fig. 12 (a) System amplitude against constant rotating forces f_o

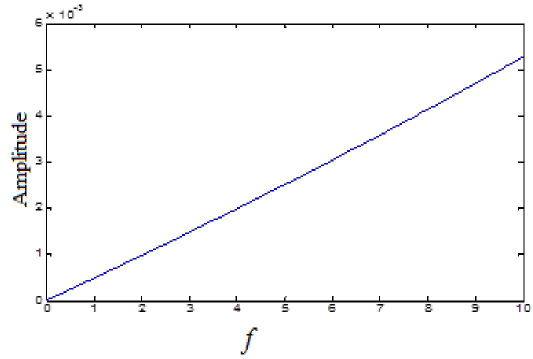

Fig. 12 (b) System amplitude against variable rotating forces f

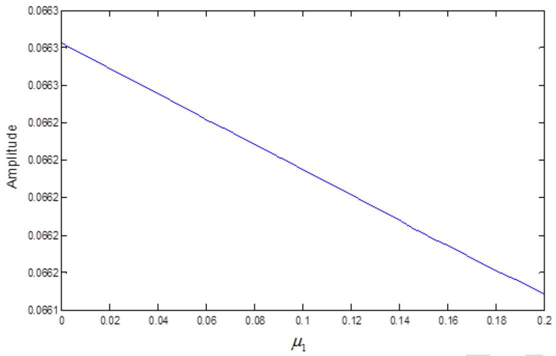

Fig. 13 (a) System amplitude against damping parameters μ_1

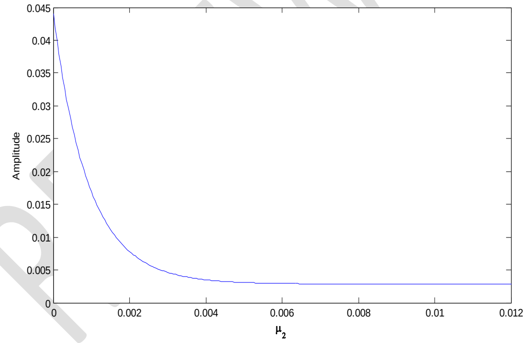

Fig. 13 (b) System amplitude against damping parameters μ_2

4Conclusions

In this research, a system of nonlinear ordinary differential equations that describing a rotating beam is analyzed approximately via multiple time scales method. We studied the effect of existence and nonexistence of the time delay on the velocity and the displacement feedback the system amplitude.The study arein case of the worst resonance cases that are primary and principal parametric resonance. We concluded that the time delay controller is more efficient than active feed-back controller on the velocity for this system, as the effective of active control is about 105%, and Time delay controller is about 125%, so the Time delay control is recommended to use in this system. The Lyapunov first method and Routh–Hurwiz criteria are adopted to achieve the stability analysis.In addition, approximate solution induced by (MSPT) is compared with numerical approximation solution using Rung-Kutta of fourth order method. The distinction offered a good agreement between approximately and numerical approaches. The effects of system parameters on the amplitude are discussed for choosing appropriate values for these parameters that attaining the system stability.

Conflict of Interest

Authors have declared that no conflict of interests in preparing this article.

Appendix

$$p_x = C_\infty \rho_\infty [\frac{a\dot{v}}{2}\sin(2\beta+2\gamma) - a\dot{u}\sin^2(\beta+\gamma) - a\dot{u}\,P\sin^3(\beta+\gamma)$$

$$-au\,P\frac{\beta_o}{L}\sin^2(\beta+\gamma)\cos(\beta+\gamma) + a\dot{v}\sin^2(\beta+\gamma)\cos(\beta+\gamma)$$

$$-av\;P\frac{\beta_o}{L}\sin^3(\beta+\gamma) - b\dot{u}\cos^2(\beta+\gamma) - \frac{b\dot{v}}{2}\sin(2\beta+2\gamma) - b\,u'P\cos^3(\beta+\gamma)$$

$$+bu\,P\frac{\beta_o}{L}\cos^2(\beta+\gamma)\sin(\beta+\gamma) - b\,v'P\cos^2(\beta+\gamma)\sin(\beta+\gamma) - b\,u\,P\frac{\beta_o}{L}\cos^3(\beta+\gamma)]$$

$$p_y = C_\infty \rho_\infty [\frac{a\dot{v}}{2}\sin(2\beta+2\gamma) - a\dot{v}\cos^2(\beta+\gamma) + au'P\sin^2(\beta+\gamma)\cos(\beta+\gamma)$$

$$+au\,P\frac{\beta_o}{L}\cos^2(\beta+\gamma)\sin(\beta+\gamma) - av'P\sin(\beta+\gamma)\cos^2(\beta+\gamma)$$

$$+av\;P\frac{\beta_o}{L}\sin^2(\beta+\gamma)\cos(\beta+\gamma) - \frac{b\,\dot{u}}{2}\sin(2\beta+2\gamma)$$

$$-b_o\dot{v}\sin^2(\beta+\gamma) - b\,u'P\cos^2(\beta+\gamma)\sin(\beta+\gamma)$$

$$+bu\,P\frac{\beta_o}{L}\cos(\beta+\gamma)\sin^2(\beta+\gamma)$$

$$-b\,v'P\cos(\beta+\gamma)\sin^2(\beta+\gamma) - bv\;P\frac{\beta_o}{L}\cos^2(\beta+\gamma)\sin(\beta+\gamma)]$$

$$a_1(z) = \oint K_{32}\frac{dx}{ds}\frac{dy}{ds} - K_{11}\,x\;y\;ds\,,$$

$$a_2(z) = \oint K_{11}\,y^2 - K_{32}\left(\frac{dx}{ds}\right)^2 ds\,,$$

$$a_3(z) = \oint K_{11}\,x^2 + K_{32}\left(\frac{dx}{ds}\right)^2 ds\,,$$

$$K_{11} = A_{22} - \frac{A_{12}^2}{A_{11}},\; K_{32} = D_{22},\; A_{ij} = \int_{-h/2}^{h/2} Q_{ij}\,dn\,,$$

$$D_{ij} = \int_{-h/2}^{h/2} Q_{ij}\,n^2\,dn\,,\; Q_{11} = Q_{22} = \frac{E}{1-\upsilon^2},$$

$$Q_{12} = Q_{21} = \frac{E\,\upsilon}{1-\upsilon^2}$$

$$\delta K = \int_0^l \left\{ b_1\left[\ddot{u} + \dot{\Omega}(R_o + z) - u\,\Omega^2\right]\delta u + b_1\ddot{v}\,\delta v \right\} dz\,,$$

$$b_1 = \oint \int_{-h/2}^{h/2} \rho\,dn\,ds\,,$$

$$W = \int_0^l \int \left(p_x\,u + p_y\,v \right) dz\,,$$

$$U = U_1 + U_2\,,$$

$$U_1=\int_0^l \rho A\,\Omega^2[R_o(L-z)+0.5(L^2-z^2)]\left[\frac{(u')^2}{2}+\frac{(v')^2}{2}\right]ds,$$

$$U_2=\frac{1}{2}\int_0^l\int\square\int_{-h/2}^{h/2}\sigma_{zz}\,\varepsilon_{zz}\,dn\,ds\,dz,$$

$$\varepsilon_{zz}=0.5\left[(u')^2+(v')^2\right]-y\,v''-x\,u''+n\left[v''\frac{dx}{ds}-u''\frac{dy}{ds}\right],$$

$$\sigma_{zz}=Q_{21}\,\varepsilon_{ss}+Q_{22}\,\varepsilon_{zz}-\alpha\,\Delta T,$$

$$\gamma_{11}=-\mu_1-\frac{\beta_5\,a_2^2\sin(2\varphi_2)}{8\omega}+\frac{\beta_{14}f^{\,2}\sin(2\varphi_1)}{8\omega}-\frac{k_2}{2},$$

$$\gamma_{12}=\frac{\beta_{14}f^{\,2}\,a_1\cos(2\varphi_1)}{4\omega}+\frac{\beta_{16}\,\Omega f\,\sin(\varphi_1)}{2\omega},$$

$$\gamma_{13}=-\frac{\beta_{13}\cos(\varphi_2)}{2}-\frac{\beta_{11}\sin(\varphi_2)}{2\omega}-\frac{\beta_5\,a_1a_2\sin(2\varphi_2)}{4\omega},$$

$$\gamma_{14}=\frac{\beta_{13}\,a_2\sin(\varphi_2)}{2}-\frac{\beta_{11}\,a_2\cos(\varphi_2)}{2\omega}-\frac{\beta_5\,a_1a_2^2\cos(2\varphi_2)}{4\omega},$$

$$\gamma_{21}=-\frac{\beta_{13}\,a_2\sin(\varphi_2)}{2a_1^2}+\frac{\beta_{11}\,a_2\cos(\varphi_2)}{2\omega a_1^2}-\frac{3\beta_5\,a_1}{4\omega}-\frac{\beta_{16}\,\Omega f\,\sin(\varphi_1)}{2\omega a_1^2},$$

$$\gamma_{22}=-\frac{\beta_{14}f^{\,2}\sin(2\varphi_1)}{4\omega}+\frac{\beta_{16}\,\Omega f\,\cos(\varphi_1)}{2\,\omega\,a_1},$$

$$\gamma_{23}=\frac{\beta_{13}\sin(\varphi_2)}{2a_1}-\frac{\beta_{11}\cos(\varphi_2)}{2\omega a_1}-\frac{\beta_5\,a_2}{2\omega}-\frac{\beta_5\,a_2\cos(2\varphi_2)}{4\omega},$$

$$\gamma_{24}=\frac{\beta_{13}\,a_2\cos(\varphi_2)}{2a_1}+\frac{\beta_{11}\,a_2\sin(\varphi_2)}{2\omega a_1}+\frac{\beta_5\,a_2^2\sin(2\varphi_2)}{4\omega},$$

$$\gamma_{31}=-\frac{\beta_{22}\cos(\varphi_2)}{2}+\frac{\beta_{21}\sin(\varphi_2)}{2\omega}+\frac{\beta_5\,a_1a_2\sin(2\varphi_2)}{4\omega},$$

$$\gamma_{32}=\frac{\beta_{24}f^{\,2}\,a_2\cos(2\varphi_2-2\varphi_1)}{4\omega},$$

$$\gamma_{33}=-\mu_2+\frac{\beta_5\,a_1^2\sin(2\varphi_2)}{8\omega}-\frac{\beta_{24}f^{\,2}\sin(2\varphi_2-2\varphi_1)}{8\omega},$$

$$\gamma_{34}=\frac{\beta_{22}\,a_1\sin(\varphi_2)}{2}+\frac{\beta_{21}\,a_1\cos(\varphi_2)}{2\omega}+\frac{\beta_5\,a_1^2\,a_2\cos(2\varphi_2)}{4\omega}-\frac{\beta_{24}f^{\,2}\,a_2\cos(2\varphi_2-2\varphi_1)}{4\omega},$$

$$\gamma_{41}=\frac{\beta_{22}\sin(\varphi_2)}{2a_2}+\frac{\beta_{21}\cos(\varphi_2)}{2\omega a_2}+\frac{\beta_5 a_1}{2\omega}(\frac{\cos(2\varphi_2)}{2}-\frac{1}{2})-\frac{\beta_{13}\ a_2\sin(\varphi_2)}{2a_1^2}$$

$$+\frac{\beta_{11}\ a_2\cos(\varphi_2)}{2\omega a_1^2}-\frac{\beta_{16}\ \Omega f\ \sin(\varphi_1)}{2\omega a_1^2},$$

$$\gamma_{42}=\frac{\beta_{24} f^{\ 2}\sin(2\varphi_1-2\varphi_2)}{4\omega}-\frac{\beta_{14} f^{\ 2}\cos(2\varphi_1)}{4\omega}+\frac{\beta_{16}\ \Omega f\ \cos(\varphi_1)}{2\omega a_1},$$

$$\gamma_{43}=-\frac{\beta_{22} a_1\sin(\varphi_2)}{2a_2^2}-\frac{\beta_{21} a_1\cos(\varphi_2)}{2\omega a_2^2}+\frac{\beta_5 a_2}{2\omega}(\frac{\cos(2\varphi_2)}{2}+\frac{1}{2})+\frac{\beta_{13}\ \sin(\varphi_2)}{2a_1}-\frac{\beta_{11}\ \cos(\varphi_2)}{2\omega a_1},$$

$$\gamma_{44}=\frac{\beta_{22} a_1\cos(\varphi_2)}{2a_2}-\frac{\beta_{21} a_1\sin(\varphi_2)}{2\omega a_2}+\frac{\beta_5\sin(2\varphi_2)}{4\omega}(a_2^2-a_1^2)-\frac{\beta_{24}\ f^{\ 2}\sin(2\varphi_1-2\varphi_2)}{4\omega}$$

$$+\frac{\beta_{13}\ a_2\cos(\varphi_2)}{2\ a_1}+\frac{\beta_{11}\ a_2\sin(\varphi_2)}{2\omega a_1},$$

$$\zeta_{11}=-\mu_1-\frac{\beta_5 a_2^2\sin(2\varphi_2)}{8\omega}+\frac{\beta_{14} f_o f\ \sin(\varphi_1)}{2\omega}-\frac{k_2}{2},$$

$$\zeta_{12}=\frac{\beta_{14} f_o f\ a_1\cos(\varphi_1)}{2\omega},$$

$$\zeta_{13}=-\frac{\beta_{13}\cos(\varphi_2)}{2}-\frac{\beta_{11}\sin(\varphi_2)}{2\omega}-\frac{\beta_5\ a_1 a_2\sin(2\varphi_2)}{4\omega},$$

$$\zeta_{14}=\frac{\beta_{13} a_2\sin(\varphi_2)}{2}-\frac{\beta_{11} a_2\cos(\varphi_2)}{2\omega}-\frac{\beta_5\ a_1 a_2^2\cos(2\varphi_2)}{4\omega},$$

$$\zeta_{21}=-\frac{\beta_{13} a_2\sin(\varphi_2)}{a_1^2}+\frac{\beta_{11} a_2\cos(\varphi_2)}{\omega a_1^2}-\frac{3\beta_5\ a_1}{2\omega},$$

$$\zeta_{22}=-\frac{\beta_{14} f_o f\ \sin(\varphi_1)}{\omega},$$

$$\zeta_{23}=\frac{\beta_{13}\sin(\varphi_2)}{a_1}-\frac{\beta_{11}\cos(\varphi_2)}{\omega a_1}-\frac{\beta_5\ a_2}{\omega}-\frac{\beta_5 a_2\cos(2\varphi_2)}{2\omega},$$

$$\zeta_{24}=\frac{\beta_{13} a_2\cos(\varphi_2)}{a_1}+\frac{\beta_{11} a_2\sin(\varphi_2)}{\omega a_1}+\frac{\beta_5 a_2^2\sin(2\varphi_2)}{2\omega},$$

$$\zeta_{31}=-\frac{\beta_{22}\cos(\varphi_2)}{2}+\frac{\beta_{21}\sin(\varphi_2)}{2\omega}+\frac{\beta_5 a_1 a_2\sin(2\varphi_2)}{4\omega},$$

$$\zeta_{32}=\frac{\beta_{24} f_o f\ a_2\cos(2\varphi_2-\varphi_1)}{2\omega},$$

$$\zeta_{33}=-\mu_2+\frac{\beta_5 a_1^2\sin(2\varphi_2)}{8\omega}+\frac{\beta_{24} f_o f\ \sin(2\varphi_2-\varphi_1)}{2\omega},$$

$$\zeta_{34}=\frac{\beta_{22} a_1\ \sin(\varphi_2)}{2}+\frac{\beta_{21} a_1\cos(\varphi_2)}{2\omega}+\frac{\beta_5 a_1^2 a_2\cos(2\varphi_2)}{4\omega}-\frac{\beta_{24} f_o f\ a_2\cos(2\varphi_2-\varphi_1)}{\omega},$$

$$\zeta_{41} = \frac{\beta_{22}\sin(\varphi_2)}{2a_2} + \frac{\beta_{21}\cos(\varphi_2)}{2\omega a_2} + \frac{\beta_5 a_1}{2\omega}\left(\frac{\cos(2\varphi_2)}{2} - \frac{1}{2}\right) - \frac{\beta_{13}\, a_2 \sin(\varphi_2)}{2a_1^2} + \frac{\beta_{11}\, a_2 \cos(\varphi_2)}{2\omega a_1^2},$$

$$\zeta_{42} = -\frac{\beta_{24} f_o f\ \sin(2\varphi_2 - \varphi_1)}{2\omega} - \frac{\beta_{14} f_o f\ \sin(\varphi_1)}{2\omega},$$

$$\zeta_{43} = -\frac{\beta_{22} a_1 \sin(\varphi_2)}{2a_2^2} - \frac{\beta_{21} a_1 \cos(\varphi_2)}{2\omega a_2^2} + \frac{\beta_5 a_2}{2\omega}\left(\frac{1}{2} - \frac{\cos(2\varphi_2)}{2}\right) + \frac{\beta_{13}\ \sin(\varphi_2)}{2a_1} - \frac{\beta_{11}\ \cos(\varphi_2)}{2\omega a_1},$$

$$\zeta_{44} = \frac{\beta_{22} a_1 \cos(\varphi_2)}{2a_2} - \frac{\beta_{21} a_1 \sin(\varphi_2)}{2\omega a_2} + \frac{\beta_5 \sin(2\varphi_2)}{4\omega}(a_2^2 - a_1^2) + \frac{\beta_{24}\ f_o f\ \sin(2\varphi_2 - \varphi_1)}{4\omega}$$

$$+ \frac{\beta_{13}\ a_2 \cos(\varphi_2)}{2a_1} + \frac{\beta_{11}\ a_2 \sin(\varphi_2)}{2\omega a_1},$$

$$\Pi_1 = -(\gamma_{11} + \gamma_{22} + \gamma_{33} + \gamma_{44}),$$

$$\Pi_2 = \gamma_{11}\gamma_{22} + \gamma_{33}\gamma_{44} + (\gamma_{11} + \gamma_{22})(\gamma_{33} + \gamma_{44})$$
$$-[\gamma_{12}\gamma_{21} + \gamma_{13}\gamma_{31} + \gamma_{14}\gamma_{41} + \gamma_{23}\gamma_{32} + \gamma_{24}\gamma_{42} + \gamma_{34}\gamma_{43}],$$

$$\Pi_3 = -\gamma_{11}[\gamma_{22}(\gamma_{33} + \gamma_{44}) - \gamma_{43} + \gamma_{33}\gamma_{44} - \gamma_{23}\gamma_{32} - \gamma_{24}\gamma_{42}) - \gamma_{22}(\gamma_{33}\gamma_{44} - \gamma_{34}\gamma_{43})$$
$$-\gamma_{23}(\gamma_{34}\gamma_{42} - \gamma_{32}\gamma_{44}) - \gamma_{24}(\gamma_{32}\gamma_{43} - \gamma_{22}\gamma_{33}) + \gamma_{12}[\gamma_{21}(\gamma_{33} + \gamma_{44}) - \gamma_{23}\gamma_{31} + \gamma_{24}\gamma_{41}]$$
$$+\gamma_{13}[\gamma_{31}(\gamma_{22} + \gamma_{44}) - \gamma_{32}\gamma_{21} - \gamma_{34}\gamma_{41}] + \gamma_{14}[\gamma_{41}(\gamma_{22} + \gamma_{33}) - \gamma_{42}\gamma_{21} - \gamma_{43}\gamma_{31}],$$

$$\Pi_4 = -\Pi_1 + \gamma_{11}[\gamma_{23}(\gamma_{34}\gamma_{42} - \gamma_{32}\gamma_{44}) + \gamma_{24}(\gamma_{43}\gamma_{32} - \gamma_{33}\gamma_{42}) - \gamma_{34}\gamma_{43}]$$
$$+\gamma_{21}\gamma_{12}(\gamma_{34}\gamma_{43} - \gamma_{33}\gamma_{44}) + \gamma_{12}\gamma_{23}(\gamma_{31}\gamma_{44} - \gamma_{34}\gamma_{41}) - \gamma_{12}\gamma_{24}(\gamma_{31}\gamma_{43} - \gamma_{33}\gamma_{41})$$
$$+\gamma_{13}[\gamma_{21}(\gamma_{32}\gamma_{44} - \gamma_{34}\gamma_{42}) + \gamma_{22}(\gamma_{34}\gamma_{41} - \gamma_{31}\gamma_{44}) + \gamma_{24}(\gamma_{31}\gamma_{42} - \gamma_{32}\gamma_{41})]$$
$$+\gamma_{14}[\gamma_{21}(\gamma_{33}\gamma_{42} - \gamma_{32}\gamma_{43}) + \gamma_{22}(\gamma_{31}\gamma_{43} - \gamma_{41}\gamma_{33}) + \gamma_{14}(\gamma_{41}\gamma_{32} - \gamma_{42}\gamma_{31})].$$

References

[1] Thomas, O., Sénéchal, A., Deü, J.-F.: Hardening/softening behavior and reduced ordermodeling of nonlinear vibrationsof rotating cantilever beams. Nonlinear Dyn. **86**, 1293–1318(2016).

[2] Zhang, X., Zhang, D., Chen, S., Hong, J.: Modal characteristics of a rotating flexible beam with a concentrated massbased on the absolute nodal coordinate formulation. NonlinearDyn. **88**, 61–77 (2017)

[3] Rezaei, M.M., Behzad, M., Haddadpour, H., Moradi, H.: Aeroelastic analysis of a rotating wind turbine blade using ageometrically exact formulation. Nonlinear Dyn. **89**, 2367– 2392 (2017).

[4] Arvin, H., Bakhtiari-Nejad, F.: Non-linear modal analysis ofa rotating beam. Int. J. Non-Linear Mech. **46**(6), 877–897(2011).

[5] Bekhoucha, F., Rechak, S., Duigou, L., Cadou, J.-M.: Nonlinear forced vibrations of rotating anisotropic beams. NonlinearDyn. **74**(4), 1281–1296 (2013).

[6] Kim, H., Chung, J.: Nonlinear modeling for dynamic analysis of a rotating cantilever beam, Nonlinear Dyn. **86**, 1981–2002 (2016).

[7] Latalski, J.: A coupled-field model of a rotating composite beam with an integrated nonlinear piezoelectric activeelement. Nonlinear Dyn. **90**, 2145–2162 (2017).

[8] Ali Kandil, Hany El-Gohary, Investigating the performance of a time delayed proportional derivative controller for rotating bladevibrations, Nonlinear Dyn 91:2631–2649 (2018).

[9] Yao, M.H., Chen, Y.P., Zhang, W.: Nonlinear vibrations of blade with varying rotating speed, Nonlinear Dyn. **68**, 487–504 (2012).

[10] Yao, M.H., Zhang, W., Chen, Y.P.: Analysis on nonlinear oscillations and resonant responses of a compressor blade,Acta Mech.,**225**, 3483–3510 (2014).

[11] Choi, S.C., Park, J.S., Kim, J.H.: Active damping of rotating composite thin-walled beams using

MFC actuators and PVDF sensors, Compos. Struct.,**76**, 362–374 (2006).
[12] Choi, S.C., Park, J.S., Kim, J.H.: Vibration control of pre-twisted rotating composite thin-walled beams with piezoelectricfiber composites, J. Sound Vib. **300**, 176–196(2007).
[13] Joy Mondal, S. Chatterjee, Controlling self-excited vibration of a nonlinear beam by nonlinear resonant velocity feedback with time-delay, International Journal of Non-Linear Mechanics **131**, 103684, (2021).
[14] Liang Li, Wei-Hsin Liao, Dingguo Zhang, Yongbin Guo, Dynamic modeling and analysis of rotating beams with partially covered enhanced active constrained layer damping treatment, Journal of Sound and Vibration, **455**, 46e68, (2019).
[15] Boumediène Chentouf, Nejib Smaoui, Exponential stabilization of a non-uniform rotating disk-beam system via a torque control and a finite memory type dynamic boundary control, Journal of the Franklin Institute **356**, 11318–11344, (2019).
[16] L.F. Lyu, W.D. Zhu, Operational modal analysis of a rotating structure under ambient excitation using a tracking continuously scanning laser Doppler vibrometer system, Mechanical Systems and Signal Processing **152**, 107367, (2021).
[17] Nayfeh, A.H., Mook, D.T.: Nonlinear Oscillations. Wiley,New York (1995).
[18] Robert L. Borrelli, Courtney S. Colman, Differential Equation, John Wiley& Sons, INC., New York, (1998).
[19] I. S. Gradshteyn and L. M. Ryzhik, 6th Ed. San Diego, Ca: Academic Press, 2000, pp. 1076.
[20] Andrea Bonito, Ricardo H. Nochetto, Dimitris Ntogkas, Discontinuous Galerkin approach to large bending deformation of a bilayer plate with isometry constraint, Journal of Computational Physics, **423**, 109785, (2020).
[21] Y. A. Amer, A. T. El-Sayed, and F. O. Darwesh, Active and Time Delay Controls on Vibrations of the MicroElectro-Mechanical System (MEMS) Resonator, Asian Research Journal of Mathematics 12(4): 1-17; Article no.ARJOM.46389 ISSN: 2456-477X, (2019).